

Modified Higgs Sectors and NLO Associated Production

Christoph Englert^a and Matthew McCullough^b

^a*Institute for Particle Physics Phenomenology, Department of Physics,
Durham University, Durham DH1 3LE, UK*

^b*Center for Theoretical Physics, Massachusetts Institute of Technology,
Cambridge, MA 02139, USA*

E-mail: christoph.englert@durham.ac.uk, mccull@mit.edu

ABSTRACT: Many beyond the Standard Model (BSM) scenarios involve Higgs couplings to additional electroweak fields. It is well established that these new fields may modify $h \rightarrow \gamma\gamma$ and $h \rightarrow \gamma Z$ decays at one-loop. However, one unexplored aspect of such scenarios is that by electroweak symmetry one should also expect modifications to the hZZ coupling at one-loop and, more generally, modifications to Higgs production and decay channels beyond tree-level. In this paper we investigate the full BSM modified electroweak corrections to associated Higgs production at both the LHC and a future lepton collider in two simple SM extensions. From both inclusive and differential NLO associated production cross sections we find BSM-NLO corrections can be as large as $\mathcal{O}(\gtrsim 10\%)$ when compared to the SM expectation, consistent with other precision electroweak measurements, even in scenarios where modifications to the Higgs diphoton rate are not significant. At the LHC such corrections are comparable to the involved QCD uncertainties. At a lepton collider the Higgs associated production cross section can be measured to high accuracy ($\mathcal{O}(1\%)$ independent of uncertainties in total width and other couplings), and such a deviation could be easily observed even if the new states remain beyond kinematic reach. This should be compared to the expected accuracy for a model-independent determination of the $h\gamma\gamma$ coupling at a lepton collider, which is $\mathcal{O}(15\%)$. This work demonstrates that precision measurements of the Higgs associated production cross section constitute a powerful probe of modified Higgs sectors and will be valuable for indirectly exploring BSM scenarios.

Contents

1	Introduction	1
2	Example BSM Scenarios	5
2.1	Vector-Like Fourth Generation Leptons	5
2.2	New Electroweak Scalars	6
3	(B)SM Electroweak Radiative Corrections at a Lepton Collider	7
3.1	SM	8
3.2	Beyond the SM	9
3.2.1	Vector-Like Fourth Generation Leptons	9
3.2.2	New Electroweak Scalars	11
3.2.3	Dominant Corrections in the Scalar Model	12
4	BSM Electroweak Radiative Corrections at the LHC	13
5	Conclusions	16

1 Introduction

Last year the ATLAS and CMS collaborations discovered a new scalar in the bosonic Higgs search channels [1, 2] exhibiting properties consistent with the Standard Model (SM) Higgs boson with mass $m_h \simeq 125$ GeV. This mass is fortuitous from both experimental and theoretical perspectives since multiple Higgs decay channels can potentially be observed, allowing for a multi-faceted exploration of electroweak symmetry breaking. The rich experimental possibilities, combined with the fact that the Higgs is the focus of many new physics scenarios, propels the Higgs to center stage in the effort to connect BSM theory with experiment. This leads to a number of phenomenologically important questions. If there is new physics, what is its nature?¹ How might we hope to observe it directly or indirectly? Addressing the latter question requires understanding in detail how new physics scenarios might affect Higgs production and decay properties and, consequently, precision analyses at present and future colliders. Even if no significant deviations in the Higgs properties are observed from the first run of the LHC, these issues remain at the top of the phenomenological agenda.

¹Due to early tentative hints for an excess in $h \rightarrow \gamma\gamma$ rates this question has stimulated a great deal of theoretical activity. See e.g. [3, 4] for explicit models and also discussions of the implications of BSM contributions to the $h\gamma\gamma$ coupling. These hints have persisted in recent ATLAS analyses [5], but only at the level of 2σ , and CMS have not yet released an updated analysis [6], so the status of this excess is very uncertain and we do not consider it a motivating factor in this work.

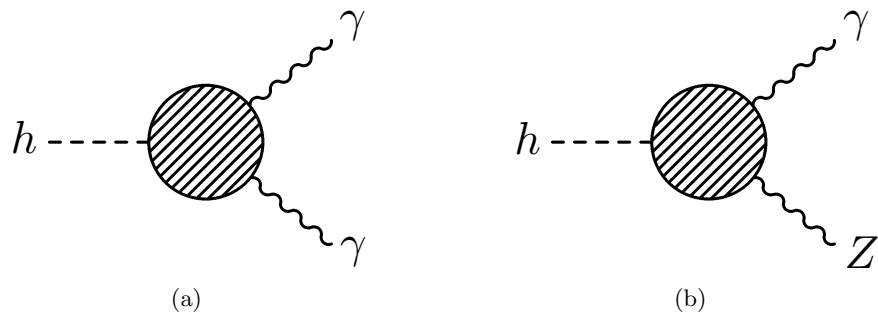


Figure 1: New electroweak-charged fields coupled to the Higgs contribute at one loop to (a) $h \rightarrow \gamma\gamma$ decays and (b) $h \rightarrow \gamma Z$ decays. The branching ratios to these final states are sensitive to the total Higgs width, which depends on Higgs couplings to other SM and BSM fields. The total rate in these channels also depends on the Higgs production cross section. Thus experimental determination of the $h\gamma\gamma$ and $h\gamma Z$ couplings, either at the LHC or a lepton collider, is subject to uncertainties in all of the Higgs couplings. For these reasons, at a 250 GeV lepton collider with 250 fb^{-1} integrated luminosity the $h\gamma\gamma$ vertex can be determined to an accuracy of $\mathcal{O}(15\%)$ [7].

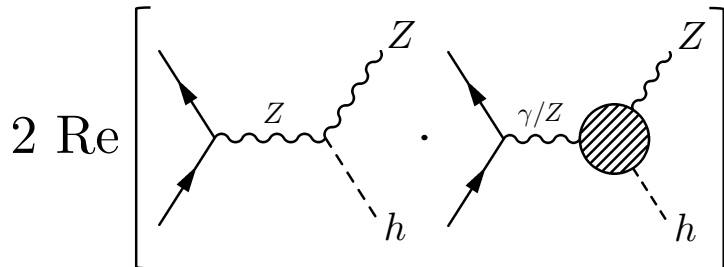


Figure 2: Higgs associated production. New electroweak-charged fields coupled to the Higgs typically contribute to this amplitude at one loop, interfering with the tree-level amplitude. The hZZ coupling can be measured to a high degree of accuracy ($\mathcal{O}(1\%)$ [7]) at a lepton collider by measuring Z -recoils in the inclusive associated production process, regardless of uncertainties regarding the total Higgs width. Hence a lepton collider gains better sensitivity to the hZZ coupling than to the $h\gamma\gamma$ and $h\gamma Z$ couplings, and opens up the possibility to discover new physics through anomalous contributions to the hZZ vertex.

Perturbative BSM scenarios which involve Higgs couplings to new electroweak fields are often characterized by new states charged under $SU(2)_L \times U(1)_Y$ which obtain, at least partially, their mass from the Higgs sector. In Figs. 1a, 1b, and 2, we schematically demonstrate that by electroweak symmetry Higgs $h \rightarrow \gamma\gamma$ decays, $h \rightarrow \gamma Z$ decays, and associated production at the Tevatron, LHC, and a future lepton collider² are typically influenced by such

²We will use the term ‘lepton collider’ in reference to any future high energy e^+e^- synchrotron, linear collider or Higgs factory.

couplings. In particular, new physics contributions that enter $h \rightarrow \gamma\gamma$ and $h \rightarrow Z\gamma$ at leading order are directly correlated with the next-to-leading order (NLO) electroweak corrections to Higgs boson production in associated production.³ This observation is not merely a technical curiosity, but is relevant across the broad scope of the experimental Higgs frontier since the associated production process lies at the heart of a number of critical measurements, which we now briefly review.⁴

While there are emerging hints of $h \rightarrow \tau\tau$ at the LHC [10, 11] and $h \rightarrow b\bar{b}$ at the Tevatron [12], the Higgs boson candidate remains to be discovered in the fermionic final states. Given that the decay $h \rightarrow b\bar{b}$ in the SM for $m_h \simeq 125$ GeV is the largest decay channel, with a branching ratio $\text{BR}_{SM}(h \rightarrow b\bar{b}) \simeq 60\%$, not observing the Higgs boson in this channel indirectly induces a large uncertainty on the extraction of Higgs couplings to other fields. We note however that this uncertainty can be artificially decreased by making assumptions on the total width of the particle. Looking to the future, observing $h \rightarrow b\bar{b}$ at the LHC in either gluon fusion or weak boson fusion will be difficult, due to overwhelmingly large QCD backgrounds, trigger issues, or the involved selection criteria which in the latter search channel typically involve central jet vetoes [1, 2, 13, 14].⁵ However, given the success of jet substructure techniques on boosted final states from associated Higgs production $pp \rightarrow hZ$ [15, 16], there is good reason to believe that such an analysis will shed light on $h \rightarrow b\bar{b}$ in the future [17–19]. Thus good theoretical control over the associated production cross section is integral to future determination of the fermionic Higgs couplings at the LHC.⁶

The status of the associated production process is elevated further at any future lepton collider since at low energies (~ 250 GeV) associated production is the dominant Higgs production process and influences all Higgs observables. Furthermore, measurements of the inclusive associated production cross section will allow determination of the hZZ coupling to $\mathcal{O}(1\%)$ accuracy, regardless of the total Higgs width, making this the most accurately determined of all the Higgs couplings. The associated production cross section also has ramifications for precision determination of a number of Higgs couplings as the total Higgs decay width can be inferred through a combination of the inclusive associated production cross section, specifically $Z \rightarrow \mu^+\mu^-$ recoiling against the Higgs, and other production and decay channels. Hence, if there are any consequences of a modified Higgs sector for associated production, they will be important at lepton colliders.

Non-decoupling parts of the one-loop contributions of Figs. 1a and 1b are sensitive to physics beyond the SM even if the new mass scale lies well above the LHC or lepton collider

³New electroweak fields will also contribute in the Z self-energy and γ/Z mixing. We include these contributions in all calculations, but not in diagrams. Similar corrections will also enter into $h \rightarrow ZZ^*$ decays. We do not consider this here, although it is certainly deserving of further investigation.

⁴For other BSM applications of the associated Higgs production process see e.g. [8, 9].

⁵Although difficult, we note that observation of $h \rightarrow b\bar{b}$ in the weak boson fusion channel is possible in the future. We thank Markus Klute for bringing this to our attention.

⁶It should also be noted that one may be able to study different production cross sections with the same Higgs decays. For example, $h \rightarrow WW^*$ decays may be observable separately in gluon fusion, vector boson fusion, and associated production channels (see e.g. [20, 21]) leading to relations between cross sections.

energy reach. If the new physics mass scale Λ is large enough, it is customary to parametrize deviations from the SM by including higher dimensional operators that arise from integrating out the dynamics above Λ in an effective field theory language.⁷ This approach has the benefit of being model independent, but is limited due to the very nature of effective field theory. This does not only follow from the non-renormalizable character of effective field theory, which systematically hinders theoretical precision [24], but sheer experimental reality puts the link between experiment and theoretical interpretation under stress. Many well-motivated physics extensions, especially in the electroweak sector, result in a phenomenology that can be consistent with current data without having a too high new physics scale $\Lambda \sim 100$ GeV. In this case, a serious drawback of the effective theory approach is that experimental signal versus background discriminating selection criteria typically need to be designed to probe momentum transfers $p_T \sim \Lambda$ simply in order to overcome the huge SM backgrounds. This means we would probe the effective theory at scales at which it cannot be considered valid. An example for such an analysis is again the boosted $h \rightarrow b\bar{b}$ associated production where $p_T(Z) \gtrsim 120$ GeV facilitates both triggering the event and rejecting the large $t\bar{t}$ +jets background [15, 16]. Therefore the precision analysis of SM extensions at similar energy scales can become model-dependent and only dedicated calculations allow one to draw a qualitatively complete picture.⁸

For the aforementioned reasons we choose to study particular models, since although one loses some degree of generality, this enables precision calculations and also serves to illustrate the features one might expect in a broader range of SM extensions. To determine where the new electroweak physics may become apparent, in this paper we investigate the correlation between two obvious observables in which new electroweak physics may lead to modifications at one-loop: corrections to $h \rightarrow \gamma\gamma$ decays, which is very commonly studied, and NLO electroweak corrections to associated Higgs production at the LHC and a future lepton collider where this cross section can be measured to high precision. To do this we employ two concrete models. We first discuss a vector-like leptonic fourth generation in Sec. 2.1 and then a charged scalar Higgs sector extension of the SM in Sec. 2.2. For both models we establish consistency with current constraints in terms of the precision electroweak S, T , and U , parameters [25, 26].

Simple electroweak extensions typically involve singlets under Quantum Chromodynamics (QCD) $SU(3)_C$. Depending on its spin, color-charged matter can compete with SM electroweak fields at one-loop, but can also be directly constrained at the LHC due to limits on the production of colored particles [27]. Discarding non-trivial color assignments, which we will do in the following, does result in some degree of qualitative theoretical deficiency, however if one wished to include colored matter then, by considering Fig. 1a, Fig. 1b, and Fig. 2, it is clear that the BSM amplitude simply scales uniformly with the casimir of the $SU(3)_C$ matter representation.

⁷For early work in the gauge and Higgs sectors see Refs. [22, 23]

⁸Note also that by typically probing a large center-of-mass energy the information encoded in electroweak precision observables such as the S, T, U observables [25, 26] do not govern the collider phenomenology.

In Sec. 3 we consider electroweak corrections at lepton colliders, at which the impact of the electroweak quantum effects is most pronounced and their observation is challenged least. We set the stage in the context of the SM in Sec. 3.1, bridging our work to the existing literature. In Sec. 3.2 we discuss modifications of the NLO electroweak phenomenology in the presence of BSM interactions. For completeness we provide a survey of the expected BSM NLO electroweak effects at the LHC in Sec. 4, utilizing exemplary parameter points that are motivated from our lepton-collider discussion of Sec. 3.2. We summarize this work and give our conclusions in Sec. 5.

2 Example BSM Scenarios

2.1 Vector-Like Fourth Generation Leptons

As a first illustrative BSM scenario we discuss a model with an additional family of vector-like leptons.⁹ The model introduces a full vector-like generation of leptons and the Lagrangian, suppressing the kinetic and gauge interactions, is¹⁰

$$-\mathcal{L} \supset m_\ell \bar{\ell}'_L \ell''_R + m_e \bar{e}'_L e'_R + m_\nu \bar{\nu}''_L \nu'_R + \text{h.c.} \quad (2.1a)$$

$$+ Y'_c (\bar{\ell}'_L H) e'_R + Y'_n (\bar{\ell}'_L i\sigma^2 H^\dagger) \nu'_R + Y''_c (\bar{\ell}''_R H) e''_L + Y''_n (\bar{\ell}''_R i\sigma^2 H^\dagger) \nu''_L + \text{h.c.} \quad (2.1b)$$

where $\ell'_L, \ell''_R = (\mathbf{2}, -1/2)$, $e'_L, e'_R = (\mathbf{1}, -1)$, and $\nu''_L, \nu'_R = (\mathbf{1}, 0)$ under $SU(2)_L \times U(1)_Y$. The left-right symmetric character of this extension guarantees cancellation of anomalies.

The parameter space of this model is large, and so we choose to make some restrictions to facilitate exploration of the relevant phenomenology. In the following we assume all vector-like masses take a common value

$$m_\ell = m_e = m_\nu = m_V \quad , \quad (2.2a)$$

where the subscript V simply denotes that this mass contribution is vector-like. We also assume that all charged fields have the same Yukawa couplings and obtain the same mass contributions from the Higgs. We make a similar simplification for the neutral fields but allow their Yukawa couplings to differ from the charged fields. Thus we define

$$Y'_c v_h / \sqrt{2} = Y''_c v_h / \sqrt{2} = m_{Ch} \quad (2.2b)$$

$$Y'_n v_h / \sqrt{2} = Y''_n v_h / \sqrt{2} = m_{Ch} + \Delta_\nu \quad , \quad (2.2c)$$

where the subscript Ch denotes that this mass contribution is chiral in nature. This simplified version of a vector-like fourth generation of leptons is hence fully specified by the parameter set $\{m_{Ch}, m_V, \Delta_\nu\}$.

⁹In Ref. [3] the model has been discussed in the context of enhanced $h \rightarrow \gamma\gamma$ decays, dark matter and constraints from direct searches.

¹⁰PMNS-like mixing of the leptons with the first three generations is quite constrained and can be avoided by imposing global symmetries. This is implicitly assumed in the following. We borrow the conventions of Ref. [3].

Finally we define m_{E_1} to be the mass of the lightest charged fermion and throughout will assume $m_{E_1} > 125$ GeV, just beyond the direct production reach of a 250 GeV lepton collider.

The mass eigenstate basis that results from diagonalizing (2.1) with (bi)unitary transformations generates mixings in the gauge and Higgs interactions (2.1b). While these mixings are important for processes involving production and decay of the new fields, they will also typically leave footprints in the low energy physics, below the energy scales at which the new physics is directly accessible. While the focus in this work is on modifications of Higgs physics at scales $\Lambda \sim m_h$, we must also consider the effects on physics at scales $\Lambda \sim m_Z$. Such modifications are conventionally expressed in terms of the precision electroweak S, T , and U , parameters [25, 26], which are sensitive to the degree of the model’s non-chirality and any additional custodial isospin violation. For our parameter identifications Eqs. (2.2a)-(2.2c), the former is controlled by m_{Ch} and the latter by Δ_ν . In the language of effective field theory, U follows from a dimension eight operator as opposed to the dimension six operators which parametrize S and T , and hence is typically suppressed [28]. In this model contributions to S and T can be considerable, and so when considering the influence of the new fields on Higgs associated production and decays we will also include precision electroweak constraints throughout.¹¹

2.2 New Electroweak Scalars

As a second illustrative BSM scenario we consider a model containing additional scalars. In particular we include an extra scalar doublet, ϕ , with the same quantum numbers as the Higgs doublet. For the sake of simplicity we assume ϕ is charged under an approximate global $U(1)$ symmetry¹² which restricts the scalar potential to contain the following terms

$$V \supset m_\phi^2 |\phi|^2 + \lambda |H|^2 |\phi|^2 + \lambda' |H \cdot \phi^\dagger|^2 . \quad (2.3)$$

After electroweak symmetry breaking the Higgs vev leads to a mass splitting between the neutral and charged scalars, ϕ_0 and ϕ_+ and also generates trilinear interactions between the Higgs and pairs of scalars. It is useful to trade the parameters of the above Lagrangian, $\{m_\phi, \lambda, \lambda'\}$, for the more intuitive set $\{m_{\phi_+}, A_{\phi_+}, \Delta_\phi\}$, where m_{ϕ_+} is the mass of the charged scalar, A_{ϕ_+} is the trilinear coupling between the Higgs and charged scalar $\mathcal{L} \supset A_{\phi_+} h |\phi_+|^2$, and Δ_ϕ is the mass splitting between the neutral and charged scalars

$$\Delta_\phi = m_{\phi_0} - m_{\phi_+} . \quad (2.4)$$

¹¹Due to the sterile neutrino extension, the model also allows additional Majorana mass terms, which can lead to a good dark matter candidate. For the present context, *i.e.* the ILC and LHC collider phenomenology at NLO, the only impact of the Majorana masses is a modified mixing of the gauge interactions, which has no effect on the observed $h \rightarrow \gamma\gamma$, and we do not consider Majorana mass terms in the following.

¹²We assume this global symmetry is broken by some small amount to allow for ϕ to decay, with the proviso that the operator responsible for this is small enough to be irrelevant for the loop corrections we discuss.

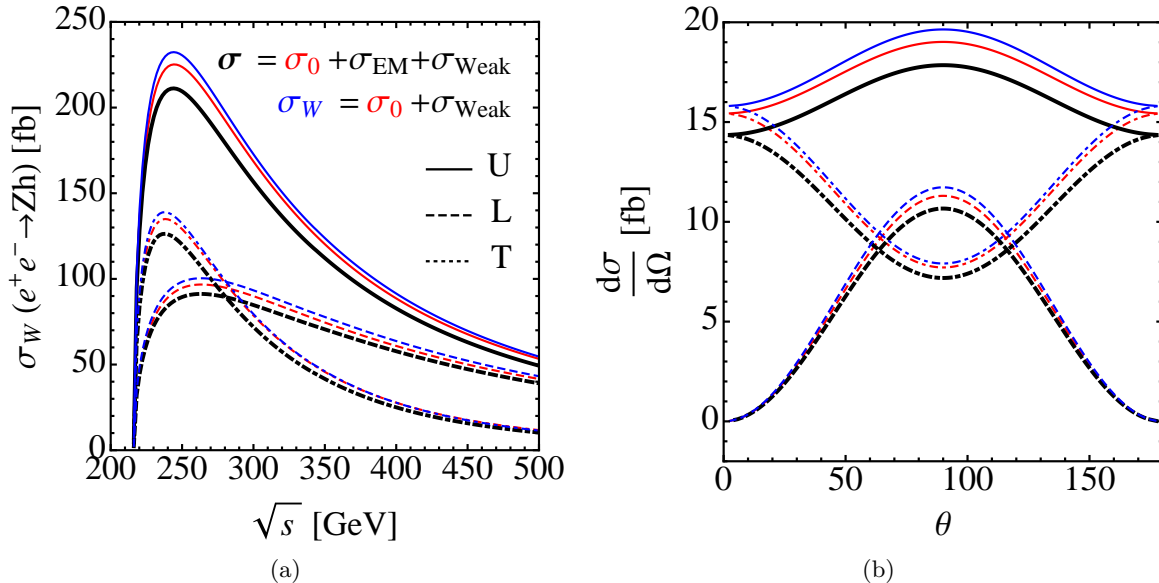


Figure 3: SM electroweak one-loop corrections to the associated production process at a lepton collider. (a) Total associated production cross section at a linear collider as a function of \sqrt{s} and (b) differential cross section at $\sqrt{s} = 250$ GeV. In both panels the tree-level result is plotted in red (middle of a set of three), the result with only weak corrections included in blue (top of three), and the full one-loop result in black (bottom of three). The various Z -boson polarizations are plotted in continuous (unpolarized), dashed (longitudinal) and dotted (transverse) lines.

As for the vector-like lepton model we will also include precision electroweak constraints on this model throughout and assume $m_{\phi_+} > 125$ GeV, such that the lightest charged scalar is beyond direct production reach at a 250 GeV lepton collider.

3 (B)SM Electroweak Radiative Corrections at a Lepton Collider

Although the Higgs was only discovered recently, the program to understand and calculate radiative corrections in various Higgs production and decay processes was initiated long ago. Measuring electroweak radiative corrections typically requires a precision machine, so in this section we focus on Higgs production at a lepton collider, and in particular consider an e^+e^- collider operating at $\sqrt{s} = 250$ GeV, for which the dominant production mechanism is associated production, $e^+e^- \rightarrow hZ$ [8, 29]. Radiative corrections to associated production at a lepton collider were calculated some time ago [30–33], and before proceeding to BSM scenarios we revisit these calculations armed with known values for the top quark and Higgs mass.

3.1 SM

Electroweak radiative corrections to $e^+e^- \rightarrow hZ$ (and also $q\bar{q} \rightarrow hZ$) consist of self energy corrections, vertex corrections and box diagrams. We follow [33] and calculate these corrections using the FEYNARTS, FORMCALC, and LOOPTOOLS packages [34, 35]. We calculate counter-terms with dimensional regularization in the complete on-mass-shell renormalization scheme [36–39] and also split the radiative corrections into two classes, electromagnetic and weak, denoting the full associated production cross section

$$\sigma = \sigma_0 + \sigma_{EM} + \sigma_{Weak} \quad , \quad (3.1)$$

where σ_0 is tree-level result, σ_{Weak} contains the weak corrections which do not involve photons within loops, and σ_{EM} includes the virtual photon correction to the eeZ vertex as well as soft photon emission. Including a massless photon in the virtual contributions of σ_{EM} we need to be inclusive on the final state to guarantee the cancellation of infrared singularities according to the Kinoshita-Lee-Nauenberg theorem [40, 41]. In the soft photon limit the real photon emission (bremsstrahlung) contribution factorizes to the born cross section [42] and we include the corresponding factor in our definition of σ_{EM} for photon energies $E(\gamma) \leq 0.1\sqrt{s}$, again following [33]. Hard photon corrections at the given order of the perturbative expansion are insensitive to new physics contributions and we do not consider them in the following; they can be vetoed in the actual analysis. To get a feeling for the magnitude of contributions coming from loops of heavy particles we can also investigate the weak corrections alone by defining

$$\sigma_W = \sigma_0 + \sigma_{Weak} \quad , \quad (3.2)$$

with the electromagnetic corrections omitted. We have verified the cancellation of UV divergences for both the weak and electromagnetic corrections and also the cancellation of IR divergences in the electromagnetic corrections.

Comparing our results with those presented in [33] we find excellent agreement. Updating with the known top-quark and Higgs mass (which we set to $m_h = 125$ GeV throughout) we calculate the weak corrections within the SM at a future 250 GeV lepton collider. In Fig. 3a we plot the total associated production cross section as a function of \sqrt{s} (which peaks near $\sqrt{s} \approx 250$ GeV) and in Fig. 3b we plot the differential cross section at $\sqrt{s} = 250$ GeV. The weak corrections are typically small and positive for all polarizations and scattering angles. The electromagnetic corrections are slightly larger and negative, thus, when combined, the weak and electromagnetic corrections lead to an overall reduction in the associated production cross section. The weak corrections remain below 5% of the tree-level cross section, and for unpolarized Z -bosons constitute an $\mathcal{O}(3\%)$ correction at $\sqrt{s} = 250$ GeV. Although these corrections are small it is expected that the hZZ coupling can be determined to $\mathcal{O}(1\%)$ accuracy at a 250 GeV lepton collider with 250 fb^{-1} integrated luminosity [7], and so weak radiative corrections can in principle be measured at such a machine.

It is clear that SM weak radiative corrections, although small, are large enough to be relevant to lepton collider Higgs studies. Their magnitude, $\mathcal{O}(3\%)$, would lead one to expect corrections arising due to perturbative BSM scenarios to be similar.

3.2 Beyond the SM

We calculate these corrections following the same methods as for the SM weak corrections and include all contributing diagrams, including those that contribute to vector boson self energies. We define the BSM correction to the associated production cross section

$$\delta\sigma_{Zh} = \frac{\sigma_{BSM}(e^+e^- \rightarrow Zh) - \sigma_{SM}(e^+e^- \rightarrow Zh)}{\sigma_0(e^+e^- \rightarrow Zh)}, \quad (3.3)$$

and in a similar manner define

$$R_{h\gamma\gamma} = \frac{\Gamma_{BSM}(h \rightarrow \gamma\gamma)}{\Gamma_{SM}(h \rightarrow \gamma\gamma)} = \frac{\text{BR}_{BSM}(h \rightarrow \gamma\gamma)}{\text{BR}_{SM}(h \rightarrow \gamma\gamma)} \left[\frac{\Gamma_{BSM}^{\text{tot}}}{\Gamma_{SM}^{\text{tot}}} \right]^{-1}. \quad (3.4)$$

Recent ATLAS fits indicate total width constraints $\Gamma_{BSM}^{\text{tot}}/\Gamma_{SM}^{\text{tot}} \lesssim 2.12$ [43]. While this number results from an overall scaling factor of LHC measurements and will therefore be limited systematically, the total Higgs width can be accessed at a 250 GeV lepton collider via a measurement of the $e^+e^- \rightarrow \nu\bar{\nu}h$ channel with subsequent decay $h \rightarrow W^+W^-$ alone at the 10% level [44]. We will assume throughout that all new fields are too heavy to introduce important new Higgs decay channels, and hence $\Gamma_{BSM}^{\text{tot}} = \Gamma_{SM}^{\text{tot}}$, such that modifications of the diphoton decay rate arise solely due to BSM contributions to the decay amplitude.

In general BSM contributions to $\delta\sigma_{Zh}$ and $R_{h\gamma\gamma}$ are correlated, however the form of this correlation is model dependent; the dependence arising through the spins and electroweak charges of the additional BSM fields. For this reason we consider this correlation in the two sample BSM scenarios described in Sec. 2.

3.2.1 Vector-Like Fourth Generation Leptons

This simplified model, presented in Sec. 2.1, is defined by the parameters $\{m_{Ch}, m_V, \Delta_\nu\}$. In each panel of Fig. 4 we fix Δ_ν to a specific value and vary m_{Ch} and m_V , plotting contours of the lightest charged fermion mass, m_{E_1} , the Higgs diphoton decay rate $R_{h\gamma\gamma}$, and corrections to the associated production cross section $\delta\sigma_{Zh}$. We also shade regions disfavored by precision electroweak measurements.

Since modifications of the Higgs diphoton decays do not involve the neutral fields, $R_{h\gamma\gamma}$ depends only on m_{Ch} and m_V . It is clear that over the majority of allowed parameter space corrections to $R_{h\gamma\gamma}$ are typically quite modest, $\mathcal{O}(10\text{'s}\%)$ compared to the $\mathcal{O}(15\%)$ model-independent experimental accuracy of the $h\gamma\gamma$ coupling. Achieving an enhancement of the diphoton decay rate requires $m_V > m_{Ch}$. This might appear surprising since this implies the dominant mass contribution does not come from the Higgs. However, if the fermion mass comes solely from the Higgs the diphoton decay rate never receives an enhancement since the contributions from loops of fermions are always smaller in magnitude and opposite in sign

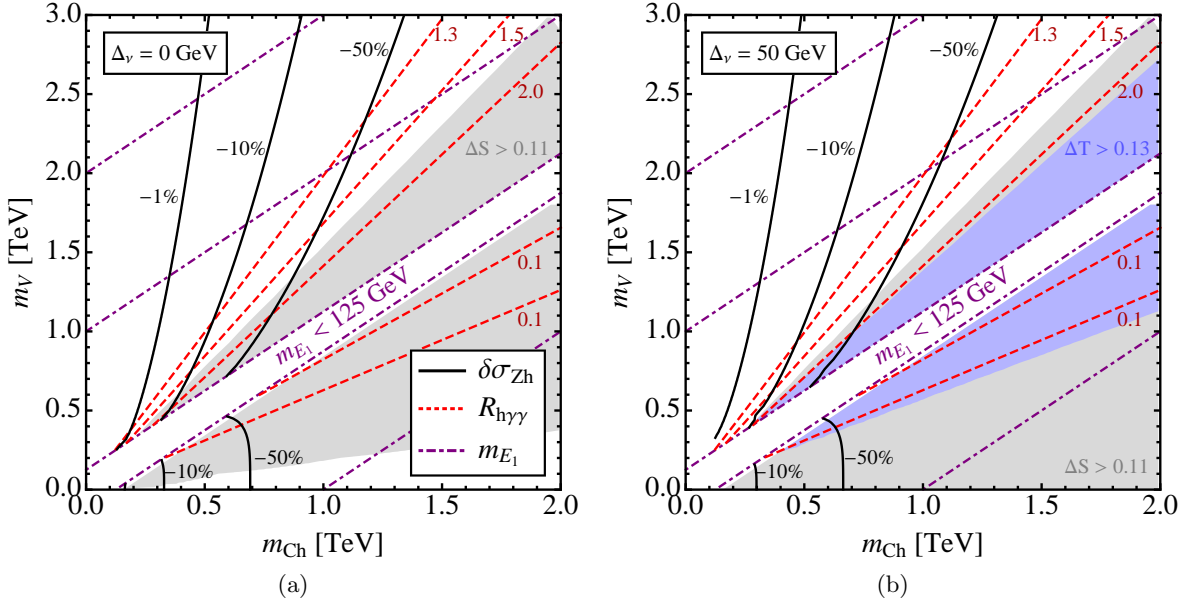


Figure 4: Contours of the modified Higgs diphoton decay rate, $R_{h\gamma\gamma}$ (dashed red), and BSM corrections to the associated production cross section $\delta\sigma_{Zh}$ (solid black) as defined in Sec. 3.2, for the vector-like fourth lepton generation model. Contours of the lightest charged fermion mass, m_{E_1} , are also shown (dotdashed purple) but not labelled. For our restricted parameter choice we have $m_{E_1} = |m_V - m_{Ch}|$ so the lightest fermion mass can be read off from the intersection of these lines with the x or y axes. (a) corresponds to the case where the Higgs contributions to charged and neutral fermion masses are equal, $\Delta_\nu = 0$ GeV, (see Eq. (2.2c)) and (b) to the case where the neutral fields couple more strongly to the Higgs than charged fermions, $\Delta_\nu = 50$ GeV. Regions where precision electroweak corrections exceed measured values by 1σ are shaded, with ΔS in gray and ΔT in blue. Parameter values where modifications to the diphoton rate are not significant (*e.g.* $\mathcal{O}(\lesssim 2\sigma)$ corresponding to the region to the left of the $R_{h\gamma\gamma} = 1.3$ contour) typically imply a reduction in the associated production which can comfortably exceed 1% compared to the SM prediction. This would be observable at a 250 GeV lepton collider which can measure this cross section to $\mathcal{O}(1\%)$ accuracy.

to the dominant amplitude from loops of W -bosons.¹³ If one increases m_V then the lightest fermion can be kept light by also increasing m_{Ch} . This then allows for much larger couplings to the Higgs for a given light fermion mass and hence a larger contribution to the Higgs diphoton amplitude.

Considering Fig. 4 it is clear that within this model BSM-NLO corrections typically lead to a reduction in the associated production cross section of 1% or greater, even in cases

¹³To achieve a large enhancement in this scenario one could always include multiple copies or larger charges, however such modifications are not within the definition of the model being studied here.

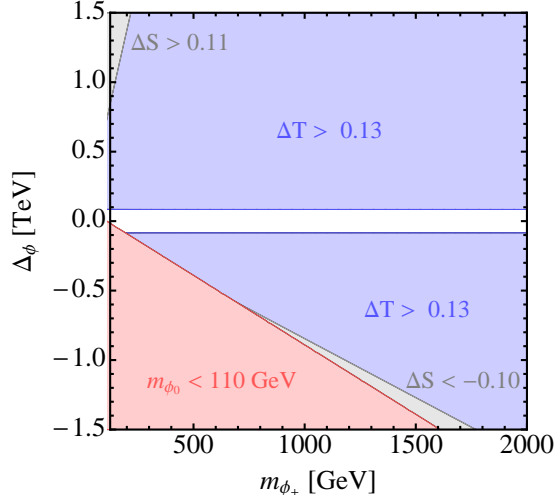


Figure 5: Precision electroweak constraints on the electroweak scalar model. By far the strongest constraint comes from the T -parameter and consistency at 1σ with precision electroweak measurements requires $|\Delta_\phi| < 84$ GeV. Inconsistency with the S -parameter only arises in small wedges of parameter space. We also require that the neutral scalar has mass greater than $m_{\phi_0} > 110$ GeV to ensure consistency with LEP bounds.

where corrections to the diphoton rate are not significant. With sensitivity to the associated production cross section at $\mathcal{O}(1\%)$ such deviations would be easily measurable at a lepton collider, even if the Higgs diphoton rate is within $\mathcal{O}(1 - 2)\sigma$ of the SM value.

Although not shown here we have also investigated the dependence of the cross section corrections on Z -boson polarizations and scattering angles. The corrections to the associated production cross section do not discriminate much between longitudinal and transverse Z -boson polarizations, with similar corrections to both. Furthermore, the corrections are also largely independent of the scattering angle.

In conclusion, if the Higgs is coupled to additional heavy charged fermions then, even if these fermions remain beyond direct collider reach, and even if their corrections to the diphoton decay rate are not significant, their presence should be evident at a lepton collider through modifications to the associated production cross section.

3.2.2 New Electroweak Scalars

This model is defined by the parameters $\{m_{\phi_+}, A_{\phi_+}, \Delta_\phi\}$ and for a particular choice of these parameters both $\delta\sigma_{Zh}$ and $R_{h\gamma\gamma}$ are completely determined. As shown in Fig. 5 the charged-neutral scalar mass splitting Δ_ϕ is constrained by precision electroweak measurements to be $|\Delta_\phi| < 84$ GeV. With this constraint imposed this model is consistent with precision electroweak measurements for the full range of m_{ϕ_+} .

In Fig. 6 we plot contours of $\delta\sigma_{Zh}$ and $R_{h\gamma\gamma}$ for fixed values of Δ_ϕ and varying values of $\{m_{\phi_+}, A_{\phi_+}\}$. From these plots it is clear that, within this particular model, it is possible

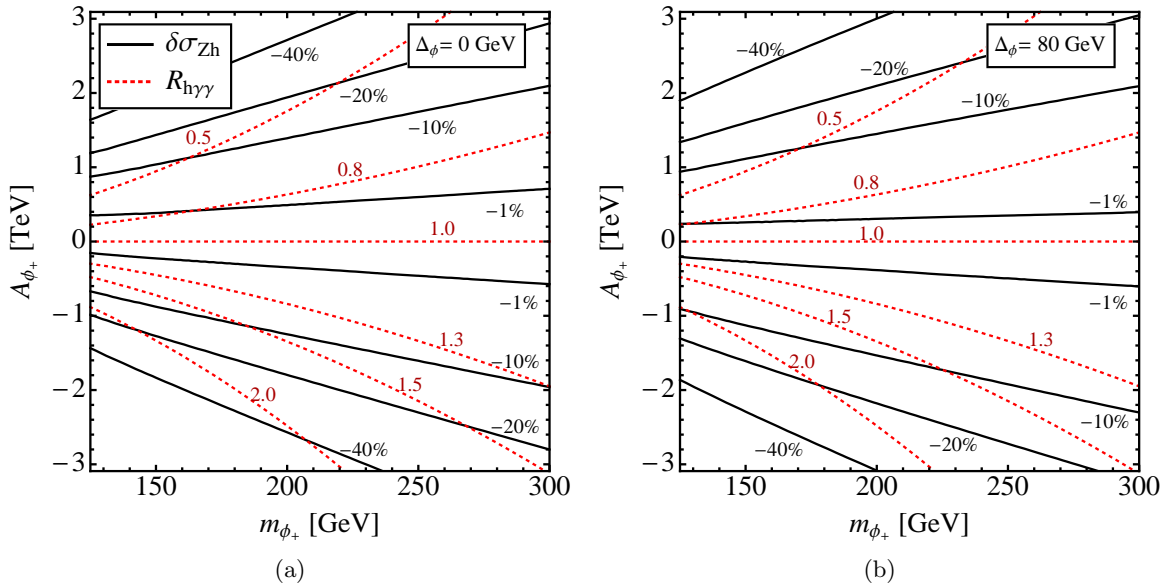


Figure 6: Contours of $\delta\sigma_{Zh}$ (see Eq. (3.3)) in solid black, and $R_{h\gamma\gamma}$ (see Eq. (3.4)) in dotted red, for the charged scalar model with varying scalar masses and Higgs couplings. Corrections to the associated production cross section are often $\mathcal{O}(\text{few})\%$ even when corrections to the diphoton rate are not significant $|R_{h\gamma\gamma} - 1| \lesssim 0.3$, (corresponding to an $\mathcal{O}(2\sigma)$ deviation in $R_{h\gamma\gamma}$). With sensitivity to the associated production cross section at the $\mathcal{O}(1\%)$ level these modifications to associate production could be observed at a linear collider.

to generate deviations in the associated production cross section which are larger than the $\mathcal{O}(1\%)$ achievable experimental resolution. Again, although not shown here, the corrections to the associated production cross section do not discriminate greatly between longitudinal and transverse Z -boson polarizations and are also largely independent of the scattering angle.

Hence, similarly to the model with vector-like fermions, if the Higgs is coupled to new charged scalars close to the weak scale then, even in the case where these scalars remain beyond direct reach of the LHC and lepton colliders, there is still the potential for measuring significant deviations in the associated production cross section at a linear collider, assuming the cross section can be measured to an accuracy of 1%.

3.2.3 Dominant Corrections in the Scalar Model

In Fig. 6 one can see that the one-loop BSM corrections, $\delta\sigma_{Zh}$, are, to a reasonable approximation, a quadratic function of the trilinear coupling A_{ϕ_+} . Of all contributing diagrams, only the scalar loops which contribute to the Higgs wavefunction renormalization have a quadratic dependence on the scalar coupling. This wavefunction renormalization then feeds into the hZZ vertex through a field redefinition to give canonically normalized external states. This contribution to the effective vertex is finite and if we only include it then modifications to the

associated production cross section can be simply written as

$$\delta\sigma_{Zh} \approx \frac{1}{16\pi^2 m_h^2} \left(A_{\phi_+}^2 G(\tau_+) + A_{\phi_0}^2 G(\tau_0) \right) , \quad (3.5)$$

where $\tau_+ = (m_h/2m_{\phi_+})^2$ and $\tau_0 = (m_h/2m_{\phi_0})^2$, which are commonly found quantities in loop integrals. A_{ϕ_+} is the trilinear coupling between the Higgs and charged scalars, as defined in Sec. 2.2, and A_{ϕ_0} is the trilinear coupling between the Higgs and neutral scalars, which can also be written as

$$A_{\phi_0} = A_{\phi_+} + \frac{2}{v_h} (m_{\phi_0}^2 - m_{\phi_+}^2) , \quad (3.6)$$

where $v_h = 246$ GeV is the usual Higgs vev. Finally we define the function

$$G(\tau) = 1 + \frac{1}{4\sqrt{\tau(\tau-1)}} \left(\log \left(1 - 2\tau - 2\sqrt{\tau(\tau-1)} \right) - \log \left(1 - 2\tau + 2\sqrt{\tau(\tau-1)} \right) \right) , \quad (3.7)$$

which is related to the derivative of the scalar two-point function. Since $0 < \tau_{+,0} < 1$ for the cases of interest the denominator and arguments of the logarithms in Eq. (3.7) are complex, however the final result is real.

Comparing with the full one-loop corrections we find that whenever the scalar coupling is large, $A_{\phi_{+,0}} \gtrsim v_h$, then Eq. (3.5) gives a reasonably good approximation to the full expression. It is interesting that the dominant one-loop correction is entirely independent of the electroweak charges of the scalars, demonstrating that the associated production cross section is a sensitive collider-probe of scenarios where the Higgs is coupled to neutral scalars via the Higgs-portal [45–52]. This is especially interesting as it applies even if the scalars are too heavy to introduce invisible decays. Thus, if there are no modifications to the Higgs diphoton decay rate, and if the Higgs has no invisible decay width, the associated production cross section can be used to probe the influence of additional neutral states at one loop.¹⁴

4 BSM Electroweak Radiative Corrections at the LHC

We now turn to a discussion of the extended electroweak corrections at the LHC. Obviously, the electroweak NLO corrections [53] are not as important as the involved higher order and resummed QCD corrections [53–59] which currently give rise to an $\mathcal{O}(10\%)$ residual perturbative uncertainty [60]. It is however not unreasonable to expect that this number will improve over time when more data becomes available and theoretical development is stimulated, such that potentially large electroweak modifications can be resolved.

Technically, we proceed along the lines of Sec. 3 to calculate the electroweak NLO corrections. We use the CTEQ611 parton distribution functions (pdfs) [61] following Ref. [53] within the VBFNLO framework [62] to handle the pdf-folding and phase space integration for $\Delta E(\gamma) \leq 0.1 \sqrt{\hat{s}}$ (\hat{s} denotes the partonic s). We have again checked the cancellations of

¹⁴As this leads to an almost universal correction to all Higgs couplings evidence for such a scenario might also arise through studying other Higgs production channels.

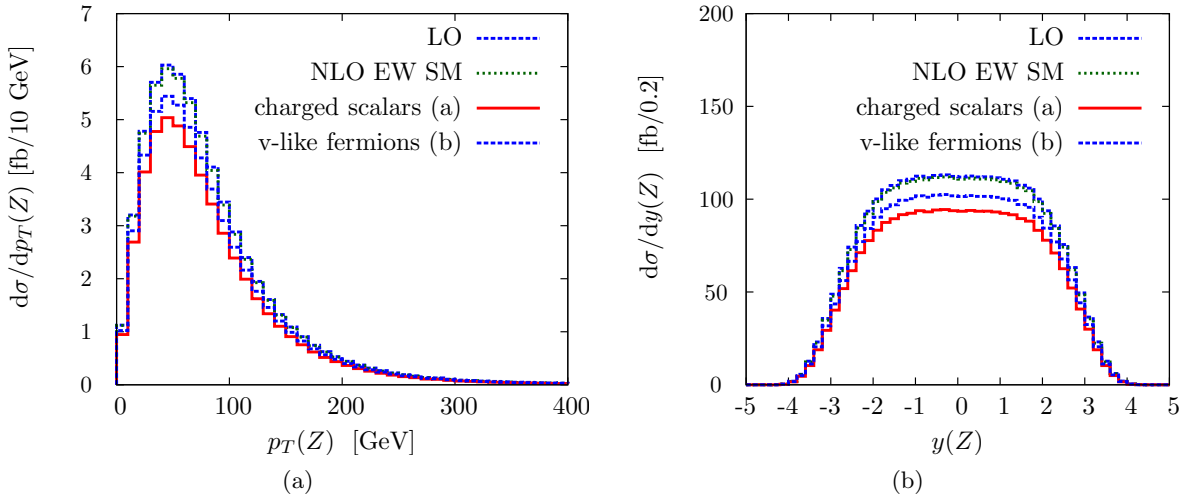


Figure 7: (a) transverse momentum, and (b) rapidity, differential distributions of the Z boson in $pp \rightarrow hZ$ production at the LHC $\sqrt{s} = 14$ TeV. We show leading order (LO) distributions as well as electroweak corrections in the SM and the BSM models discussed in the previous sections. The BSM parameter choices are given in Eq. (4.1) and Eq. (4.3). The integrated cross section receives corrections $\delta\sigma_{Zh} \simeq -15\%$ in the charged scalar model and $\delta\sigma_{Zh} \simeq -8\%$ in the vector-like fermion model. The correction relative to the SM value, as a function of p_T , is shown separately in Fig. 8.

both UV and IR singularities and we find excellent agreement comparing to integrated results from FORMCALC/LOOPTOOLS which validates our phase space integration. Our leading order matrix element has been cross checked against MADGRAPH [63] for individual phase space points.¹⁵

As done for the e^+e^- case we regulate the soft photon divergencies with a slicing parameter which is equivalent to dimensional regularization [64], and we do not consider either initial state photon contributions or hard photon corrections.¹⁶

In Fig. 7 we show differential distributions for the SM and our BSM scenarios. For a $2 \rightarrow 2$ scattering process the most relevant distributions are transverse momentum p_T and rapidity y . Dependence on the azimuthal angle, Φ , is trivial. The remaining collider observables follow as functions of (p_T, y, Φ) and the involved masses m_Z, m_h .

¹⁵Electroweak processes also typically depend on the electroweak scheme that is used to construct the parameters of the electroweak sector from a minimal set of observables [53]. This dependence can be large but is not important for us since it does not involve the BSM contributions.

¹⁶In principle, the presence of collinear mass singularities requires extending the list of subprocesses to photon-induced processes and the DGLAP kernels accordingly. Such pdf sets exist, see *e.g.* Ref. [65], but their contribution to the present process is known to be negligible $< 1\%$ for our purposes [66, 67]. Note that none of these contributions is sensitive to the BSM extension that we study. The full treatment will not change our results; especially the adoption of Eq. (3.3) to the LHC situation is insensitive to all non-BSM effects.

The charged scalar mass scenarios we will study in the following are given by

$$(a) \quad (m_{\phi_+}, A_{\phi_+}, \Delta_\phi) = (250 \text{ GeV}, -2.0 \text{ TeV}, 80 \text{ GeV}) , \quad (4.1)$$

$$(a') \quad (m_{\phi_+}, A_{\phi_+}, \Delta_\phi) = (250 \text{ GeV}, +0.7 \text{ TeV}, 80 \text{ GeV}) , \quad (4.2)$$

and we choose a parameter point for the vector-like lepton scenario

$$(b) \quad (m_{Ch}, m_V, \Delta_\nu) = (500 \text{ GeV}, 1000 \text{ GeV}, 0 \text{ GeV}) . \quad (4.3)$$

These parameter points are motivated from our results of Sec. 3.2, Figs. 4 and 6. We choose (a) and (b) in the lepton collider $\{R_{h\gamma\gamma}, \sigma(hZ)\}$ correlation such that the diphoton decay rate takes an extreme value $R_{h\gamma\gamma} \simeq 1.5$, while (a') is a parameter point with a $\sim 20\%$ decrease in $R_{h\gamma\gamma}$ compared to the SM.¹⁷

We find LHC BSM cross sections $\delta\sigma(hZ) \simeq -15\%, -8\%$ for the parameter and model choices (a) and (b), respectively. For (a') we obtain $\delta\sigma(hZ) \simeq -1\%$. These numbers qualitatively reproduce the lepton collider results of Sec. 3.2 (we remind the reader that $\delta\sigma$ is mostly driven by the BSM corrections). As in the lepton collider case, the scalar extension shows a larger deviation as compared to the fermion model. The scalar model is also less constrained by electroweak precision results, which follows from a formal decoupling of the non-oblique corrections (see also Sec. 3.2.3).

In Fig. 8 we show the phase space dependence in terms of the Z boson transverse momentum, which is sensitive to the BSM contributions, especially when we start probing the new physics mass scale. This justifies our choice to work in concrete models as compared to effective theories mentioned in the introduction. This effect is more clearly visible in Fig. 8. The total cross section is dominated from low p_T configurations, yet for analyses where associated production is accompanied with a high p_T cut, such as in $h \rightarrow b\bar{b}$ where $p_T(Z) \simeq 150 \text{ GeV}$, we observe a turn-on of the new physics contribution which further decreases the cross section compared to the SM expectation on the inclusive level. The phase space dependence of the correction, however, is highly dependent on the model. The overall effect is small and in the percent range, but should nonetheless be considered in precision studies that aim to determine Higgs properties at the

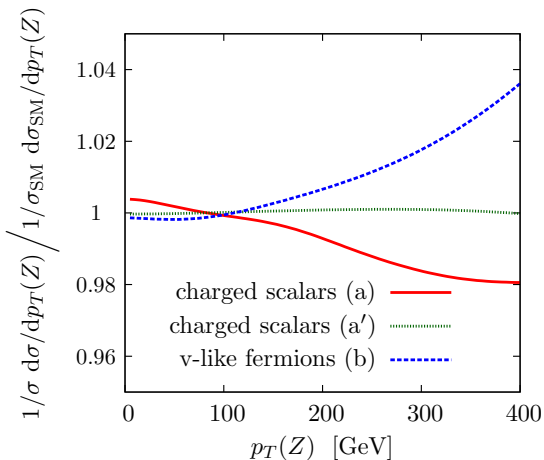


Figure 8: Phase space dependence of the BSM electroweak corrections of the considered models and parameter points as a function of the Z boson transverse momentum.

¹⁷The fourth generation vector-like lepton model does not admit $R_{h\gamma\gamma} < 1$ due to electroweak precision constraints

LHC. Within the context of the charged scalar model the parameter point (a') does not result in important effects on LHC associated production.

We have only discussed $pp \rightarrow hZ$ but expect our results should generalize to $pp \rightarrow hW^\pm$ qualitatively as in the SM [53], and so these results also have relevance for the $pp \rightarrow hW \rightarrow WWW$ channel [20].

5 Conclusions

In this work we have investigated the higher order electroweak corrections to associated Higgs production at a future lepton collider and the LHC in electroweak extensions of the Higgs sector. Because higher order corrections are model and phase space dependent, we have studied them within two simple BSM scenarios which involve vector-like leptons and charged scalars. Our results are of importance for the consideration of Higgs physics at a future lepton collider since couplings and branching ratios can be measured to high precision. Reconciling the new physics contributions with current limits from LEP measurements we find regions of parameter space with $\mathcal{O}(10\%)$ or larger deviations of the Higgs associated production cross section, in comparison to the SM expectation. These corrections are much larger than the expected lepton collider precision, and are possible even when corrections to the diphoton rate are within $\mathcal{O}(1 - 2)\sigma$ of the expected precision.

We find similar corrections for LHC collisions. The phase space dependence is typically such that the integrated BSM cross section modifications are dominated by soft events, but high p_T events exhibit the largest deviations. These corrections, when compared to the SM, can again be $\mathcal{O}(10\%)$, which might be resolvable for high luminosity studies. The phase space dependence of the BSM contribution then becomes a non-negligible parameter in precision cross section and coupling extractions, which, depending on the data, might challenge an effective field theory based analysis as *de facto* considered in Ref. [68].

While signals for any BSM physics at the LHC remain elusive it is increasingly important to explore the full breadth of potential experimental BSM signatures. Although the direct observation of new BSM states still remains a possibility, it may be that indirect evidence in the form of anomalous properties of SM states and processes might also uncover new physics. Since many well-motivated BSM scenarios are concerned with the Higgs sector, the newly discovered Higgs then becomes, perhaps, the strongest candidate for indirect hints of new physics and it is timely to understand the full complement of possible BSM modifications to its properties. This effort is already underway with intense study in various respects, however this work highlights that as we progress into the Higgs precision era it is important that theoretical progress in SM precision Higgs calculations comes accompanied by BSM precision Higgs calculations. The scope of BSM precision Higgs physics is extensive and in this work we have only considered corrections to Higgs associated production in two simplified models. However, this has demonstrated that if the Higgs is coupled to new electroweak states then there exist regions of parameter space where modifications to $h \rightarrow \gamma\gamma$ rates may remain

below statistical significance, while corrections to associated production, particularly at a lepton collider, may in fact lead to the most significant evidence for a modified Higgs sector.

Acknowledgements

We thank Markus Klute for conversations and for comments on an early version of the draft. M.M. has benefitted from conversations with Jesse Thaler and Itay Yavin. C.E. acknowledges funding by the Durham International Junior Research Fellowship scheme. M.M. is supported by a Simons Postdoctoral Fellowship and by the U.S. Department of Energy (DOE) under cooperative research agreement DE-FG02-05ER-41360.

References

- [1] The ATLAS collaboration, *Observation of a new particle in the search for the Standard Model Higgs boson with the ATLAS detector at the LHC*, *Phys.Lett.* **B716** (2012) 1–29, [[arXiv:1207.7214](#)].
- [2] The CMS collaboration, *Observation of a new boson at a mass of 125 GeV with the CMS experiment at the LHC*, *Phys.Lett.* **B716** (2012) 30–61, [[arXiv:1207.7235](#)].
- [3] A. Joglekar, P. Schwaller, and C. E. Wagner, *Dark Matter and Enhanced Higgs to Di-photon Rate from Vector-like Leptons*, *JHEP* **1212** (2012) 064, [[arXiv:1207.4235](#)].
- [4] Djouadi, *Phys.Lett.* **B435** (1998) 101–108. Petriello, *JHEP* **0205** (2002) 003. Han, Logan, McElrath, and L.-T. Wang, *Phys.Lett.* **B563** (2003) 191–202. Chen, Tobe, and Yuan, *Phys.Lett.* **B640** (2006) 263–271. Low and Shalgar, *JHEP* **0904** (2009) 09. Cacciapaglia, Deandrea, and Llodra-Perez, *JHEP* **0906** (2009) 054. Low, Rattazzi, and Vichi, *JHEP* **1004** (2010) 126. Casagrande, Goertz, Haisch, Neubert, and Pfoh, *JHEP* **1009** (2010) 014. Englert, Plehn, Zerwas and Zerwas, *Phys. Lett.* **B703** (2011) 298. Cao, Heng, Liu, and M. Yang, *Phys.Lett.* **B703** (2011) 462–468. Alves, Ramirez Barreto, Dias, Pires, Queiroz, *et. al.*, *Phys.Rev.* **D84** (2011) 115004. Carena, Gori, Shah, and Wagner, *JHEP* **1203** (2012)014. Arvanitaki and Villadoro, *JHEP* **1202** (2012)144. Batell, Gori, and Wang, *JHEP* **1206** (2012)172. Kanemura and Yagyu, *Phys.Rev.* **D85** (2012)115009. Barger, Ishida, and Keung, *Phys.Rev.Lett.* **108** (2012) 261801. Draper and McKeen, *Phys.Rev.* **D85** (2012)115023. Dawson and Furlan, *Phys.Rev.* **D86** (2012)01502. Arhrib, Benbrik, and Chen, [1205.5536](#). Carena, Gori, Shah, Wagner, and Wang, *JHEP* **1207** (2012)175. Akeroyd and Moretti, *Phys.Rev.* **D86** (2012)035015. Carena, Low, and Wagner, *JHEP* **1208** (2012) 060. Chang, Ng, and Wu, *Phys.Rev.* **D86** (2012) 033003. Bellazzini, Petersson, and Torre, *Phys.Rev.* **D86** (2012) 033016. Ke, Luo, Shan, Wang, and Wang, *Phys.Lett.* **B718** (2013) 1334–1341. Low, Lykken, and Shaughnessy, *Phys.Rev.* **D86** (2012) 093012. Chiang and Yagyu, [1207.1065](#). Giardino, Kannike, Raidal, and Strumia, *Phys.Lett.* **B718** (2012) 469–474. Buckley and Hooper, *Phys.Rev.* **D86** (2012) 075008. Carmi, Falkowski, Kuflik, Volansky, and Zupan, *JHEP* **1210** (2012) 196. An, Liu, and Wang, *Phys.Rev.* **D86** (2012) 075030. Alves, Dias, Barreto, Pires, Queiroz, *et. al.*, [1207.3699](#). Abe, Chen, and He, *JHEP* **1301** (2013) 082. Bertolini and McCullough, *JHEP* **1212** (2012) 118. Joglekar, Schwaller, and Wagner, *JHEP* **1212** (2012) 064. Arkani-Hamed, Blum, D’Agnolo, and Fan, [1207.4482](#). Haba, Kaneta, Mimura, and Takahashi, *Phys.Lett.***B718** (2013) 1441–1446. Almeida, Bertuzzo, Machado, and Funchal,

- JHEP* **1211** (2012) 085. Alves, Fox, and Weiner, [1207.5499](#). Batell, McKeen, and Pospelov, *JHEP* **1210** (2012) 104. Giudice, Paradisi, and Strumia, *JHEP* **1210** (2012) 186. Delgado, Nardini, and Quiros, *Phys.Rev.* **D86** (2012) 115010. Kearney, Pierce, and Weiner, *Phys.Rev.* **D86** (2012) 113005. Hashimoto and Miransky, *Phys.Rev.* **D86** (2012) 095018. Schmidt-Hoberg and Staub, *JHEP* **1210** (2012) 195. Reece, [1208.1765](#). Davoudiasl, Lee, and Marciano, *Phys.Rev.* **D86** (2012) 095009. Cai, Chao, and Yang, *JHEP* **1212** (2012) 043. Bae, Jung, and Kim, *Phys.Rev.* **D87**(2013) 015014. Voloshin, *Phys.Rev.* **D86** (2012) 093016. Kitahara, *JHEP* **1211** (2012) 021. Kobakhidze, [1208.5180](#). Urbano, [1208.5782](#). Chun, Lee, and Sharma, *JHEP* **1211** (2012) 106. Lee, Park, and Park, *JHEP* **1212** (2012) 037. Batell, Gori, and Wang, [1209.6382](#). Altmannshofer, Gori, and Kribs, *Phys.Rev.* **D86** (2012) 115009. Chala, *JHEP* **1301** (2013) 122. Picek and Radovic, [1210.6449](#). Choi, Im, Jeong, and Yamaguchi, [1211.0875](#). Batell, Jung, and Lee, [1211.2449](#). Schmidt-Hoberg, Staub, and Winkler, *JHEP* **1301** (2013) 124. Davoudiasl, Lewis, and Ponton, [1211.3449](#). Dissauer, Frandsen, Hapola, and Sannino, [1211.5144](#). Carena, Gori, Low, Shah, and Wagner, [1211.6136](#). Berg, Buchberger, Ghilencea, and Petersson, [1212.5009](#). Iltan, [1212.5695](#). Han, Liu, Wu, Yang, and Zhang, [1212.6728](#). Chao, Zhang, and Zhang, [1212.6272](#). Funatsu, Hatanaka, Hosotani, Orikasa, and Shimotani, [1301.1744](#). Kang, Liu, and Ning, [1301.2204](#). Fan and Reece, [1301.2597](#). Cao, Wu, Wu, and Yang, [1301.4641](#). Chen, Geng, Huang, and Tsai, [1301.4694](#). Feng and Nath, [1303.0289](#)
- [5] The ATLAS collaboration, *Latest ATLAS studies on Higgs to diboson states*, Rencontres de Moriond 2013, EW session, March 2-9.
- [6] The CMS collaboration, *Study of Standard Model Scalar Production in Bosonic Decay Channels in CMS*, Rencontres de Moriond 2013, EW session, March 2-9.
- [7] M. Klute, R. Lafaye, T. Plehn, M. Rauch, and D. Zerwas, *Measuring Higgs Couplings at a Linear Collider*, [arXiv:1301.1322](#).
- [8] W. Kilian, M. Kramer, and P. Zerwas, *Anomalous couplings in the Higgsstrahlung process*, *Phys.Lett.* **B381** (1996) 243–247, [[hep-ph/9603409](#)].
- [9] J. Ellis, V. Sanz, and T. You, *Associated Production Evidence against Higgs Impostors and Anomalous Couplings*, [arXiv:1303.0208](#).
- [10] The ATLAS collaboration, *Updated ATLAS results on the signal strength of the Higgs-like boson for decays into WW and heavy fermion final states*, *ATLAS-CONF* **2012-162** (2012).
- [11] The CMS collaboration, *Combination of Standard Model Higgs boson searches and measurements of the properties of the new boson with a mass near 125 GeV*, *CMS-HIG* **12-045** (2012).
- [12] **TEVNPH (Tevatron New Phenomena and Higgs Working Group), CDF Collaboration, D0 Collaboration** Collaboration, *Combined CDF and D0 Search for Standard Model Higgs Boson Production with up to 10.0 fb⁻¹ of Data*, [arXiv:1203.3774](#).
- [13] Y. L. Dokshitzer, V. A. Khoze, and T. Sjostrand, *Rapidity gaps in Higgs production*, *Phys.Lett.* **B274** (1992) 116–121.
- [14] V. D. Barger, R. Phillips, and D. Zeppenfeld, *Mini - jet veto: A Tool for the heavy Higgs search at the LHC*, *Phys.Lett.* **B346** (1995) 106–114, [[hep-ph/9412276](#)].

- [15] J. M. Butterworth, A. R. Davison, M. Rubin, and G. P. Salam, *Jet substructure as a new Higgs search channel at the LHC*, *Phys.Rev.Lett.* **100** (2008) 242001, [[arXiv:0802.2470](#)].
- [16] D. E. Soper and M. Spannowsky, *Combining subjet algorithms to enhance ZH detection at the LHC*, *JHEP* **1008** (2010) 029, [[arXiv:1005.0417](#)].
- [17] The CMS collaboration, *Search for the standard model Higgs boson decaying to bottom quarks in pp collisions at $\sqrt{s} = 7$ TeV*, *Phys.Lett.* **B710** (2012) 284–306, [[arXiv:1202.4195](#)].
- [18] The ATLAS collaboration, *Search for the Standard Model Higgs boson produced in association with a vector boson and decaying to a b-quark pair with the ATLAS detector*, *Phys.Lett.* **B718** (2012) 369–390, [[arXiv:1207.0210](#)].
- [19] The ATLAS collaboration, *ATLAS Sensitivity Prospects for 1 Higgs Boson Production at the LHC Running at 7, 8 or 9 TeV*, *ATL-PHYS-PUB* **2010-015** (2010).
- [20] The CMS collaboration, *Search for SM Higgs in WH to WWW to 3l 3n*, *CMS-PAS-HIG-12-039*.
- [21] The CMS collaboration, *Evidence for a particle decaying to W+W- in the fully leptonic final state in a standard model Higgs boson search in pp collisions at the LHC*, *CMS-PAS-HIG-12-042*.
- [22] K. Hagiwara, R. Peccei, D. Zeppenfeld, and K. Hikasa, *Probing the Weak Boson Sector in $e^+e^- \rightarrow W^+W^-$* , *Nucl.Phys.* **B282** (1987) 253.
- [23] W. Buchmuller and D. Wyler, *Effective Lagrangian Analysis of New Interactions and Flavor Conservation*, *Nucl.Phys.* **B268** (1986) 621.
- [24] G. Passarino, *NLO Inspired Effective Lagrangians for Higgs Physics*, *Nucl.Phys.* **B868** (2013) 416–458, [[arXiv:1209.5538](#)].
- [25] M. E. Peskin and T. Takeuchi, *A New constraint on a strongly interacting Higgs sector*, *Phys.Rev.Lett.* **65** (1990) 964–967.
- [26] M. E. Peskin and T. Takeuchi, *Estimation of oblique electroweak corrections*, *Phys.Rev.* **D46** (1992) 381–409.
- [27] The ATLAS collaboration, *Search for new phenomena in the dijet mass distribution updated using 13.0 fb^{-1} of pp collisions at $\sqrt{s} = 8$ tev collected by the atlas detector*, Tech. Rep. ATLAS-CONF-2012-148, CERN, Geneva, Nov, 2012.
- [28] R. Barbieri, A. Pomarol, R. Rattazzi, and A. Strumia, *Electroweak symmetry breaking after LEP-1 and LEP-2*, *Nucl.Phys.* **B703** (2004) 127–146, [[hep-ph/0405040](#)].
- [29] W. Kilian, M. Kramer, and P. Zerwas, *Higgsstrahlung and W W fusion in e+ e- collisions*, *Phys.Lett.* **B373** (1996) 135–140, [[hep-ph/9512355](#)].
- [30] J. Fleischer and F. Jegerlehner, *RADIATIVE CORRECTIONS TO HIGGS PRODUCTION BY e+ e- to Z H IN THE WEINBERG-SALAM MODEL*, *Nucl.Phys.* **B216** (1983) 469.
- [31] F. Jegerlehner, *ELECTROWEAK RADIATIVE CORRECTIONS IN THE HIGGS SECTOR*.
- [32] J. Fleischer and F. Jegerlehner, *O (alpha) CORRECTIONS TO HIGGS PRODUCTION PROCESSES AT LEP ENERGIES*, .

- [33] A. Denner, J. Kublbeck, R. Mertig, and M. Bohm, *Electroweak radiative corrections to $e^+ e^-$ to $H Z$* , *Z.Phys.* **C56** (1992) 261–272.
- [34] T. Hahn, *Generating Feynman diagrams and amplitudes with FeynArts 3*, *Comput.Phys.Commun.* **140** (2001) 418–431, [[hep-ph/0012260](#)].
- [35] T. Hahn and M. Perez-Victoria, *Automatized one loop calculations in four-dimensions and D-dimensions*, *Comput.Phys.Commun.* **118** (1999) 153–165, [[hep-ph/9807565](#)].
- [36] A. Denner, *Techniques for calculation of electroweak radiative corrections at the one loop level and results for W physics at LEP-200*, *Fortsch.Phys.* **41** (1993) 307–420, [[arXiv:0709.1075](#)].
- [37] K.-i. Aoki, Z. Hioki, R. Kawabe, M. Konuma, and T. Muta, *ELECTROWEAK RADIATIVE CORRECTIONS TO HIGH-ENERGY neutrino e SCATTERINGS*, *Prog.Theor.Phys.* **65** (1981) 1001.
- [38] K.-i. Aoki, Z. Hioki, R. Kawabe, M. Konuma, and T. Muta, *ONE LOOP CORRECTIONS TO neutrino e SCATTERING IN WEINBERG-SALAM THEORY: NEUTRAL CURRENT PROCESSES*, *Prog.Theor.Phys.* **64** (1980) 707.
- [39] K. Aoki, Z. Hioki, M. Konuma, R. Kawabe, and T. Muta, *Electroweak Theory. Framework of On-Shell Renormalization and Study of Higher Order Effects*, *Prog.Theor.Phys.Suppl.* **73** (1982) 1–225.
- [40] T. Lee and M. Nauenberg, *Degenerate Systems and Mass Singularities*, *Phys.Rev.* **133** (1964) B1549–B1562.
- [41] T. Kinoshita, *Mass singularities of Feynman amplitudes*, *J.Math.Phys.* **3** (1962) 650–677.
- [42] G. Bonneau and F. Martin, *Hard photon emission in $e^+ e^-$ reactions*, *Nucl.Phys.* **B27** (1971) 381–397.
- [43] The ATLAS collaboration, *Coupling properties of the new higgs-like boson observed with the atlas detector at the lhc*, Tech. Rep. ATLAS-CONF-2013-011, CERN, Geneva, Sep, 2012.
- [44] C. F. Duerig, *Determination of the Higgs Decay Width at ILC*. PhD thesis, University of Bonn, 2012.
- [45] V. Silveira and A. Zee, *SCALAR PHANTOMS*, *Phys.Lett.* **B161** (1985) 136.
- [46] J. McDonald, *Gauge singlet scalars as cold dark matter*, *Phys.Rev.* **D50** (1994) 3637–3649, [[hep-ph/0702143](#)].
- [47] C. Burgess, M. Pospelov, and T. ter Veldhuis, *The Minimal model of nonbaryonic dark matter: A Singlet scalar*, *Nucl.Phys.* **B619** (2001) 709–728, [[hep-ph/0011335](#)].
- [48] H. Davoudiasl, R. Kitano, T. Li, and H. Murayama, *The New minimal standard model*, *Phys.Lett.* **B609** (2005) 117–123, [[hep-ph/0405097](#)].
- [49] B. Patt and F. Wilczek, *Higgs-field portal into hidden sectors*, [hep-ph/0605188](#).
- [50] R. Schabinger and J. D. Wells, *A Minimal spontaneously broken hidden sector and its impact on Higgs boson physics at the large hadron collider*, *Phys. Rev.* **D72** (2005) 093007, [[hep-ph/0509209](#)].
- [51] T. Binoth and J. J. van der Bij, *Influence of strongly coupled, hidden scalars on Higgs signals*, *Z. Phys.* **C75** (1997) 17, [[hep-ph/9608245](#)].

- [52] C. Englert, T. Plehn, M. Rauch, D. Zerwas and P. M. Zerwas, *LHC: Standard Higgs and Hidden Higgs*, *Phys. Lett.* **B707** (2012) 512, [[arXiv:1106.3097](#)].
- [53] M. Ciccolini, S. Dittmaier, and M. Kramer, *Electroweak radiative corrections to associated WH and ZH production at hadron colliders*, *Phys.Rev.* **D68** (2003) 073003, [[hep-ph/0306234](#)].
- [54] J. Ohnemus and W. J. Stirling, *Order alpha-s corrections to the differential cross-section for the W H intermediate mass Higgs signal*, *Phys.Rev.* **D47** (1993) 2722–2729.
- [55] H. Baer, B. Bailey, and J. Owens, *O (alpha-s) Monte Carlo approach to W + Higgs associated production at hadron supercolliders*, *Phys.Rev.* **D47** (1993) 2730–2734.
- [56] T. Han and S. Willenbrock, *QCD correction to the pp → WH and ZH total cross-sections*, *Phys.Lett.* **B273** (1991) 167–172.
- [57] O. Brein, A. Djouadi, and R. Harlander, *NNLO QCD corrections to the Higgs-strahlung processes at hadron colliders*, *Phys.Lett.* **B579** (2004) 149–156, [[hep-ph/0307206](#)].
- [58] R. Hamberg, W. van Neerven, and T. Matsuura, *A Complete calculation of the order α_s^2 correction to the Drell-Yan K factor*, *Nucl.Phys.* **B359** (1991) 343–405.
- [59] S. Dawson, T. Han, W. Lai, A. Leibovich, and I. Lewis, *Resummation Effects in Vector-Boson and Higgs Associated Production*, *Phys.Rev.* **D86** (2012) 074007, [[arXiv:1207.4207](#)].
- [60] **LHC Higgs Cross Section Working Group** Collaboration, S. Dittmaier *et. al.*, *Handbook of LHC Higgs Cross Sections: 1. Inclusive Observables*, [arXiv:1101.0593](#).
- [61] J. Pumplin, D. Stump, J. Huston, H. Lai, P. M. Nadolsky, *et. al.*, *New generation of parton distributions with uncertainties from global QCD analysis*, *JHEP* **0207** (2002) 012, [[hep-ph/0201195](#)].
- [62] K. Arnold, M. Bahr, G. Bozzi, F. Campanario, C. Englert, *et. al.*, *VBFNLO: A Parton level Monte Carlo for processes with electroweak bosons*, *Comput.Phys.Commun.* **180** (2009) 1661–1670, [[arXiv:0811.4559](#)].
- [63] J. Alwall, P. Demin, S. de Visscher, R. Frederix, M. Herquet, *et. al.*, *MadGraph/MadEvent v4: The New Web Generation*, *JHEP* **0709** (2007) 028, [[arXiv:0706.2334](#)].
- [64] U. Baur, S. Keller, and D. Wackerroth, *Electroweak radiative corrections to W boson production in hadronic collisions*, *Phys.Rev.* **D59** (1999) 013002, [[hep-ph/9807417](#)].
- [65] A. Martin, R. Roberts, W. Stirling, and R. Thorne, *Parton distributions incorporating QED contributions*, *Eur.Phys.J.* **C39** (2005) 155–161, [[hep-ph/0411040](#)].
- [66] J. Kripfganz and H. Perlt, *ELECTROWEAK RADIATIVE CORRECTIONS AND QUARK MASS SINGULARITIES*, *Z.Phys.* **C41** (1988) 319–321.
- [67] H. Spiesberger, *QED radiative corrections for parton distributions*, *Phys.Rev.* **D52** (1995) 4936–4940, [[hep-ph/9412286](#)].
- [68] The ATLAS collaboration, *Coupling properties of the new higgs-like boson observed with the atlas detector at the lhc*, Tech. Rep. ATLAS-CONF-2012-127, CERN, Geneva, Sep, 2012.